Neural Variability in Premotor Cortex Provides a Signature of Motor Preparation
J. Neurosci. Churchland et al. 26: 3697

Supplemental data

Files in this Data Supplement:

- Supplementary figure 1. Analysis of EMG activity. A. EMG records obtained from the deltoid of monkey B, with one subplot for reaches to each of seven directions ('fast' reaches to an 85 mm distant red target). Each subplot shows median EMG signal (thin solid traces) and the mean +/- the standard error of the EMG signal (shaded region). To indicate where the movement began and ended, the dashed lines plot mean hand speed in the direction of the target. An EMG signal of zero would plot directly on top of the initial segment of the speed traces, but the scaling is otherwise arbitrary. Two epochs are shown: the first aligned to target onset (arrow) and the second to movement onset. B. EMG records obtained for the one recording that did show a noteworthy (though small) change in activity during the delay: the trapezius of monkey B.

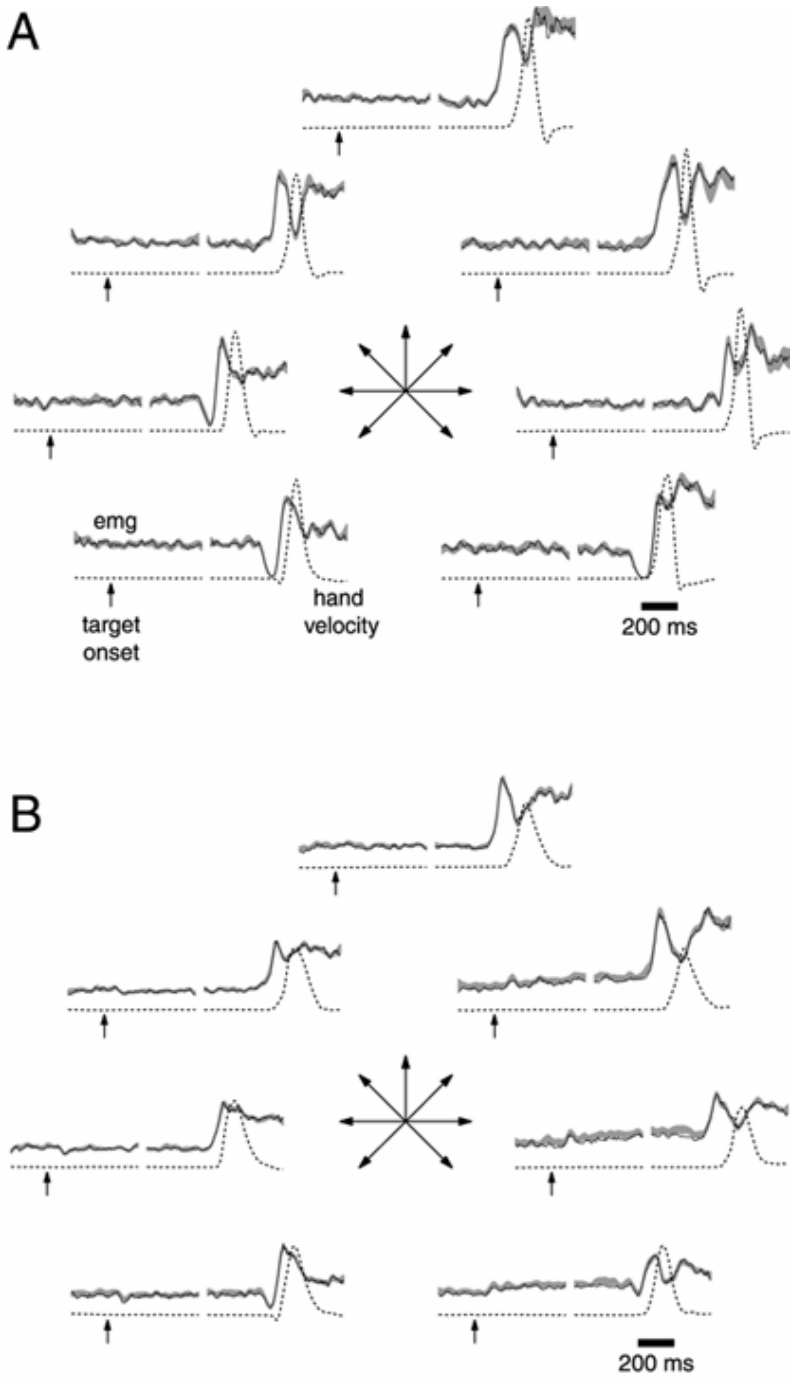

supplementary figure 1

- Supplementary figure 2. Further analysis of changes in variability, under conditions where analysis is restricted to target locations that evoked little change in response (same data and selection as in Figure 8B,C). A. Mean firing rate as a function of time (same as in Figure 8B, but on an expanded scale) is plotted relative to baseline (horizontal line). B. The un-normalized variance, with flanking traces giving the standard error across isolations/target-locations. Due to the lack of normalization, variability tends to track the changes in mean firing rate (being higher for higher firing rates, as expected from a Poisson process). This is true even though the changes in mean firing rate (A) are modest. However, one can still observe a strong trend towards lower variability later in the trial. Comparing different time-points with similar mean firing rates (e.g. the two dashed lines) variability is lower later in the trial (e.g. 133 ± 8 and 102 ± 6 spikes2/s2 for those two points). Thus, the drop in variability is visible even in the un-normalized variance, although this measure is generally problematic because it is influenced by changes in the mean rate. This was, of course, the reason for using the normalized variance in the first place. However, we note that it is possible to correct for the expected influence of mean firing rate without normalizing, by computing the variance minus the mean C. The variance minus the mean. When computing this difference, the mean was first multiplied by a scaling factor (k = 9.14 spikes/s, see methods) that accounts for the effect of filtering, so that the expected value of the variance minus the mean is zero for a Poisson process. The assumption made by this method (that the intrinsic variability to be 'factored-out' is Poisson) is less forgiving than that made when computing the NV (that the intrinsic variance is linearly related to the mean firing rate, but not necessarily with unity slope). However, this concern is not great, given that the firing rates in this analysis are changing little to begin with. Indeed, computing the variance minus the mean gives much the same result as computing the NV. These analyses were also applied to data from the other two monkeys, with similar results.

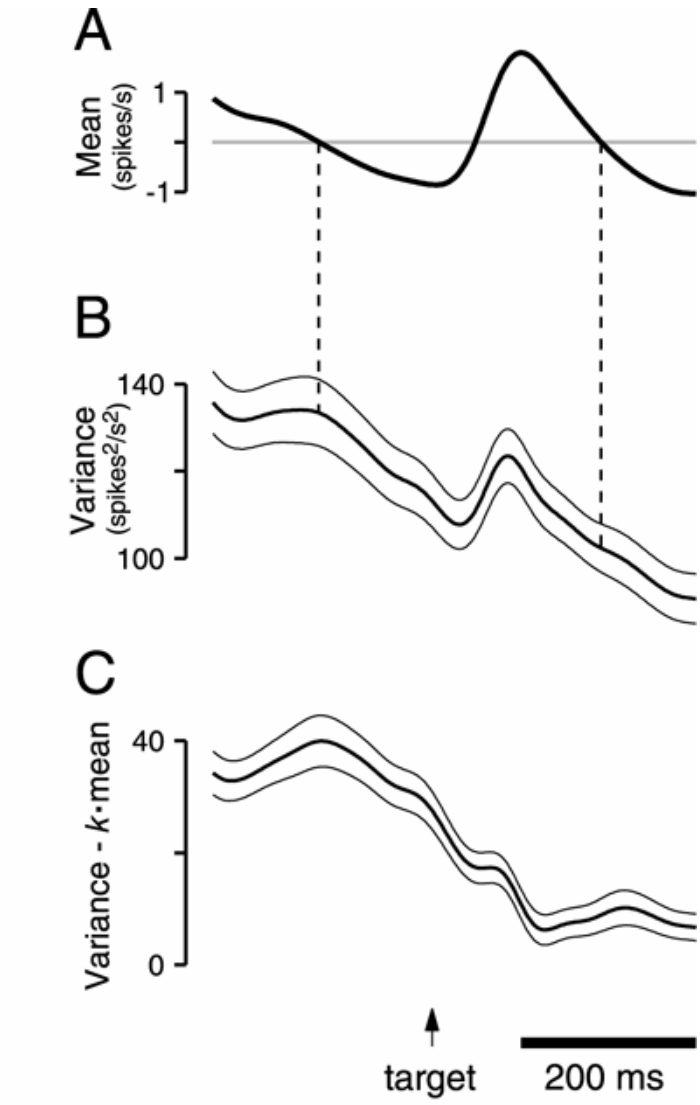

supplementary figure 2

- Supplementary figure 3. Analysis of across-trial covariance for monkey G. Target onset and the go cue are indicated by the black arrow and the vertical grey line. The top trace plots the change in firing rate (from baseline) as a function of time, averaged across all isolations and target locations (preferred and non-preferred). The middle trace plots the NV. The bottom trace plots the covariance, computed as described in the Methods. Flanking traces show standard errors of the mean. Data are from an experiment using three discrete delay durations, but only data from the 230 ms delay are analyzed here, allowing analysis to be simultaneously locked to target onset and the go cue. Further analysis of this same dataset is shown in Fig. 9. Note that for this dataset, fixation remained near the central spot for the duration of the delay. We also applied this analysis to the dataset in Figure 6A. Results were very similar to those presented above: a large drop was seen in the covariance, in contrast to the expectation if neurons came to share a central rhythm.

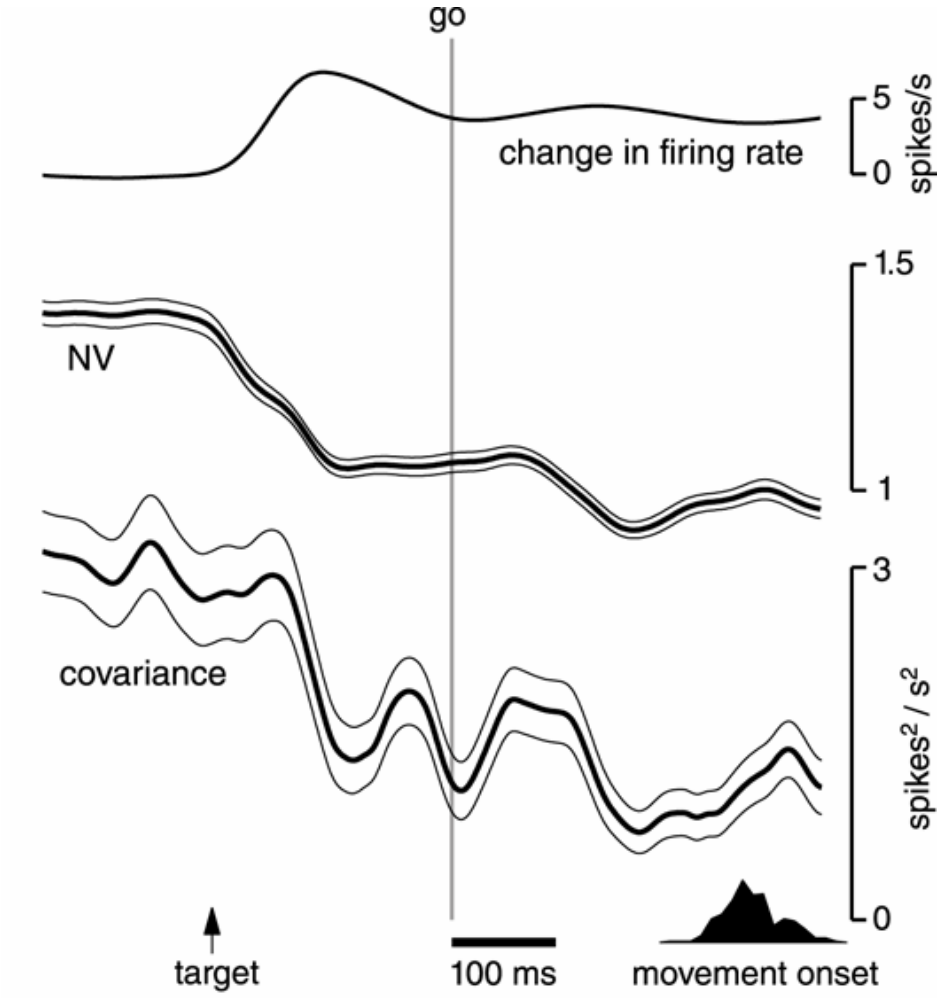

supplementary figure 3

- Supplementary figure 4. Re-analysis of Fig. 9A (230 ms delay-period), using different filters for the initial smoothing of spike-trains. Each panel shows the mean change (from baseline) in firing rate (top) and the mean NV (bottom), averaged across all isolations and target locations, with flanking SEMs. Data are aligned to target onset, and thus also to the go cue. The solid circle at the bottom of each panel plots the mean time of movement onset. A. The analysis was performed using a Gaussian with a 30 ms standard deviation, as was done originally. B. Using a Gaussian with a 15 ms standard deviation. C. Using a +/- 30 ms box filter. This method of computing the NV is mathematically identical to computing the Fano-factor using a 60 ms sliding window. D. Using a +/- 10 ms box filter, equivalent to the Fano-factor with a 20 ms sliding window. Note that shorter filters (panels B and D) lead to lower magnitudes of the main effect compared to longer filters (panels A and C). This is expected. For a truly Poisson process, the value of the NV (or the Fano-factor) will not depend on filter length. However, when statistics depart from Poisson, the magnitude of the departure from unity does depend on the filter length. Indeed, changes in the Fano-factor with window duration have been previously observed (Oram et al. 2001; Averbeck and Lee 2003, Osborne et al. 2004). The relevant observation here is that, even for the shorter filters, the decline in the NV still consumes at least 100 ms.

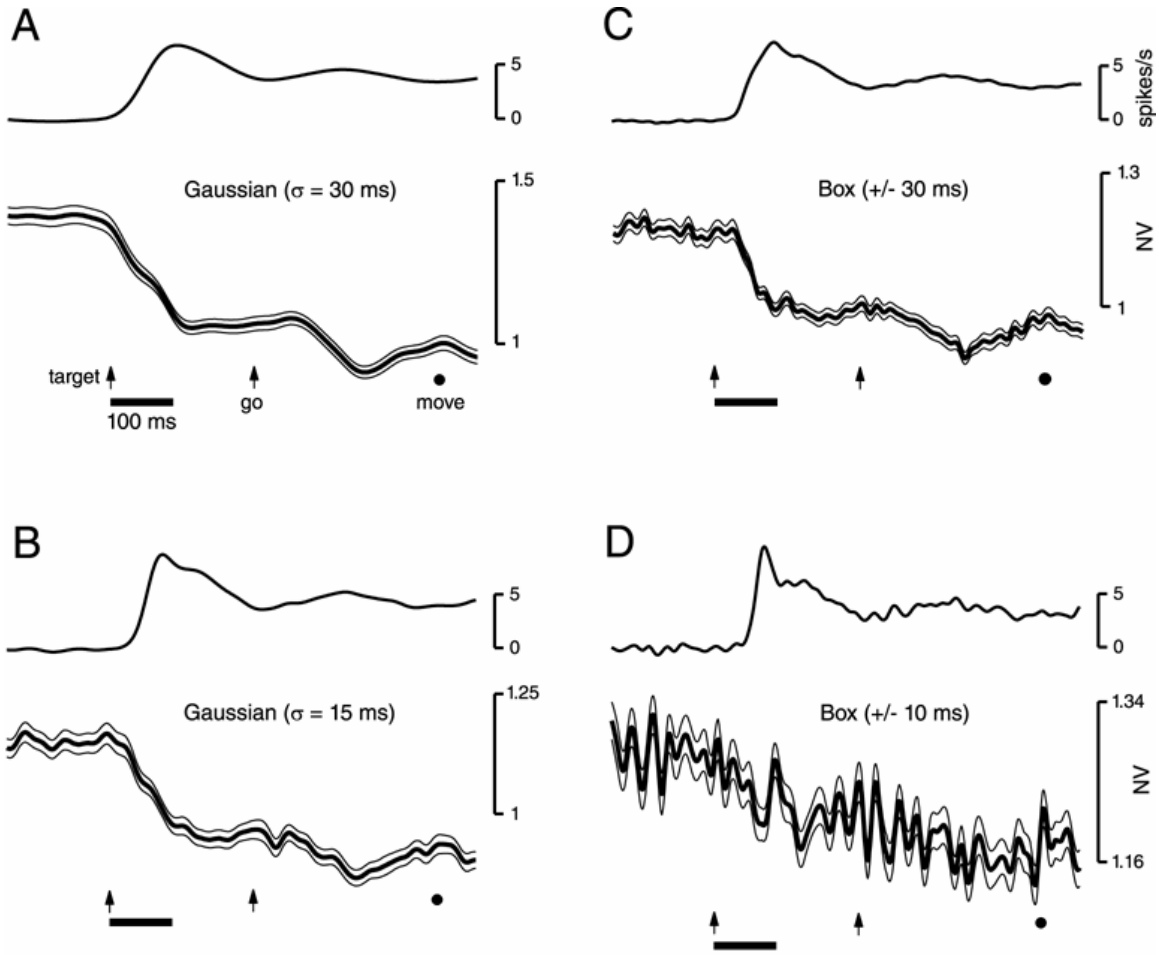

supplementary figure 4